AN EMPIRICAL APPROACH TO TOKAMAK TRANSPORT

R.J. Hawryluk

Princeton University, Plasma Physics Laboratory, Princeton, P.O. Box 451, NJ 08544 USA

ABSTRACT

This lecture will present an overview of the important considerations related to particle and energy transport in a tokamak. Transport in tokamaks can be inferred by analyzing the experimental data in terms of the one dimensional magnetic field diffusion equation and the particle and energy conservation equations. This approach will be illustrated by considering current penetration during the startup phase, density buildup in high density discharges, as well as the ion and electron energy balance in PLT ohmically heated discharges. Areas requiring further research will be discussed.

INTRODUCTION

Two complementary approaches exist in analyzing tokamak data in order to infer the underlying transport processes. The first is to use a one dimensional transport code to simulate the tokamak discharge, such as that used by Duchs, Post and Rutherford (1976) and Post and coworkers (1978). In this approach, either the predictions of a theoretical transport model are compared with experimental data or an empirical transport model is derived by iteration on the assumed transport (and often impurity) model in order to obtain an acceptable fit to the experimental data. One advantage of this approach is that the computed results are always internally consistent. Another is that after a theoretical model has been verified or an empirical model derived, it is very easy to extrapolate to other conditions. This is especially useful in perdicting the performance of future devices. The disadvantage of this approach is that it is often difficult to isolate a single facet of the problem. For example, in trying to understand current penetration during the startup phase, it is necessary to predict the electron temperature and density profiles accurately in order to calculate the plasma conductivity, $\sigma(r,t)$. It is simpler and more reliable to use the measured profiles directly to calculate $\sigma(r,t)$.

This in fact is what is done in the second approach which utilizies a transport analysis code. In this approach, whenever possible, experimental data are used directly to calculate local transport coefficients. Some quantities, for instance the current density, $j(r)$, and neutral density, $n_o(r)$, profiles are very difficult to measure and thus are not typically available . For these parameters, models very similar to those used in the one dimensional simulation codes, are used to supplement the measured data. The advantage of this second approach is that the interpretation of the data is more direct and comparison with theoretical models is straightforward. Clearly, this approach places a heavy burden on the reliability of the data and understanding of the limitations of a particular diagnostic. However, even in the first approach, the validity and the associated confidence level of the inferred transport model is determined by the uncertainty in the data used for comparison.

This lecture will describe the transport analysis code which has been developed by R. J. Goldston, D. McCune, G. L. Schmidt and myself. This code will be used here mainly as a pedagogical tool to illustrate various important processes related to cross-field transport. In particular, current penetration during the startup phase, particle fluxes in high density He discharges, and the ion and electron energy balance in ohmically heated PLT discharges will be discussed. In the workshop Dr. Goldston will use this code to discuss the analysis of neutral beam injected discharges. Throughout this lecture, many important questions which remain to be satisfactorily resolved will be pointed out.

TRANSPORT ANALYSIS CODE

The general structure of the time dependent transport analysis code which has been used to analyze PLT and PDX ohmically heated discharges is shown in Fig. 1. The experimental measurements are used to solve the magnetic field diffusion equation, calculate the neutral density profile and then using the particle and energy conservation equations calculate the local transport coefficients. This approach will be presented in detail later in the lecture. At this point, only an overview will be given to show how the various calculations are related.

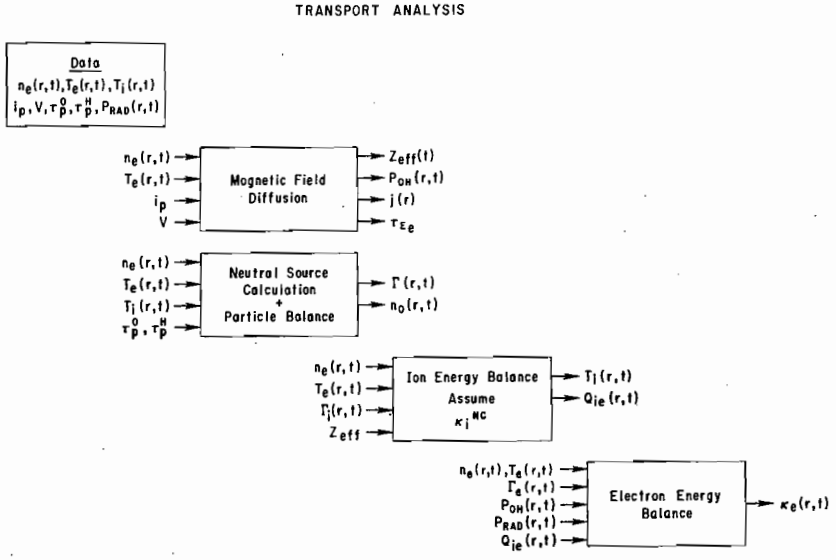

Fig. 1. Illustrates the structure of the transport analysis code.

The data inputs to the code include plasma current, i_p, surface voltage, V, and spectroscopic measurements of hydrogen and impurity confinement times (τ_p^H and τ_p^0) in addition to profile measurements of electron density $n_e(r,t)$, electron temperature, $T_e(r,t)$, ion temperature, $T_i(r,t)$, and the radiated power, $p_{rad}(r,t)$. The electron density and temperature profiles are obtained by the multichannel Thomson scattering system (Bretz and coworkers, 1978). The ion temperature profile are from measurements of the charge exchange flux, neutron emission and Doppler broadening of impurity lines (Brusati and coworkers, 1978). The power radiated is from bolometric measurements (Hsuan and coworkers, 1978).

On the basis of the measurements, the code solves the magnetic field diffusion equation for the poloidal magnetic field, $B_\theta(r,t)$ in order to evaluate $Z_{eff}(t)$, and the current density, $j(r,t)$. From these quantities, the ohmic input power, $p_{OH}(r,t)$, the electron energy confinement time, τ_{Ee} and the safety factor q are calculated. (The electron energy confinement time is defined as the electron energy divided by the ohmic input power, neglecting the rate of change of the electron energy.)

In the next stage, the neutral density and temperature profiles are calculated on the basis of the particle confinement time measurements in order to determine the radial particle flux from the particle conservation equation. The particle confinement time is defined as the total number of particles in the discharge divided by the total flux of particles to the walls and limiters.

Two approaches can be used to investigate the ion energy balance. The preferred approach would be to calculate the ion heat conduction from the ion temperature profiles, and the inferred electron-ion heat transfer, charge exchange loss and particle convection. Then, the deduced ion heat conduction would be compared with the neoclassical prediction. However, because detailed ion temperature profiles are not always available, the ion temperature profile is calculated assuming neoclassical ion heat conduction. The power loss due to convection is obtained from the inferred particle flux and the charge exchange loss from the neutral penetration calculation. This approach is a generically similar to the time independent calculations of Stott (1976), Brusati and coworkers (1978), and Equipe TFR (1978).

Finally, the electron heat conduction is deduced from the electron energy balance equation. The inputs to the calculation are the measured electron density and temperature profiles, and radiated power and the deduced ohmic input power, electron-ion transfer and the power loss due to convection. This power loss is obtained from the inferred electron fluxes.

MAGNETIC FIELD DIFFUSION

In this section, two questions will be considered. First, can current penetration during the startup phase be modeled by a one dimensional magnetic field diffusion code assuming neoclassical conductivity? Second, what are the uncertainties in the subsequent calculations of the electron energy balance in the quasi-steady state due to uncertainties in the plasma resistivity?

Current Penetration[1]

Current penetration during the startup phase of PLT was investigated by solving the one dimensional poloidal magnetic field diffusion equation,

$$\frac{\partial B_\theta}{\partial t} = \frac{\partial}{\partial r}\left(\frac{1}{r\mu_o\sigma(r,t)}\frac{\partial}{\partial r}rB_\theta\right), \tag{1}$$

subject to the usual boundary conditions:

$$B_\theta(0) = 0 \tag{1a}$$

and

$$B_\theta(a) = \frac{\mu_o i_p}{2\pi a}, \tag{1b}$$

[1]The results discussed in this section are from a study by R. J. Hawryluk, N. Bretz, D. Dimock, E. Hinnov, D. Johnson, D. McCune, D. Monticello and S. Suckewer.

The analytic approximation of Hirshman, Hawryluk and Birge (1977) was used to calculate the neoclassical conductivity

$$\sigma(r,t) = \sigma_o \Lambda_e(Z_{eff}) \left(1 - \frac{f_t}{1+\epsilon\nu_{*e}}\right) \left(1 - \frac{C_R(Z_{eff})f_t}{1+\epsilon\nu_{*e}}\right) . \qquad (2)$$

The two terms on the right hand side correspond to the neoclassical correction where f_t is the fraction of trapped particles and ν_{*e} is the electron collisionality parameter. As $f_t \Rightarrow 0$ or $\nu_{*e} \Rightarrow \infty$, the neoclassical conductivity goes to its classical limit, $\sigma_o \Lambda_e(Z_{eff})$. In the calculation of $\sigma(r,t)$, Z_{eff} is assumed to be independent of minor radius and the magnitude of Z_{eff} is adjusted by iteration to obtain agreement with the measured surface voltage. In this manner, the enhancement required in the neoclassical resistivity to account for the current penetration during the startup phase is evaluated.

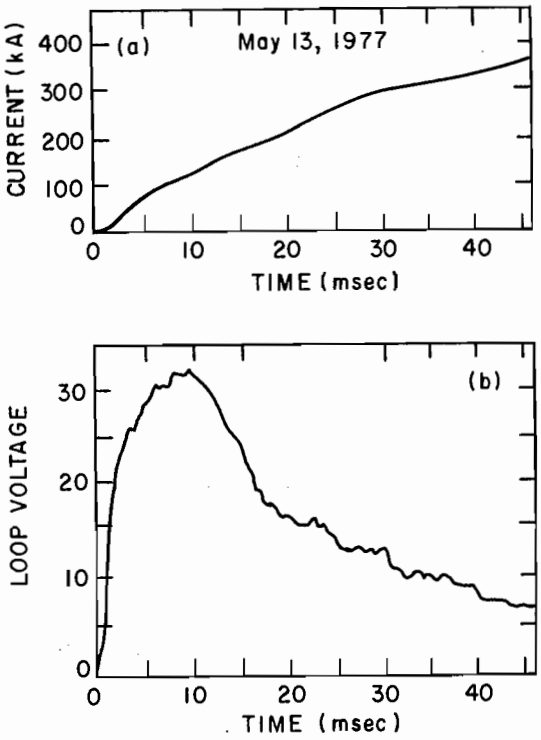

Fig. 2. Plasma current and loop voltage as measured across the ceramic break on the vacuum vessel during the startup phase of a high density He discharge in PLT.

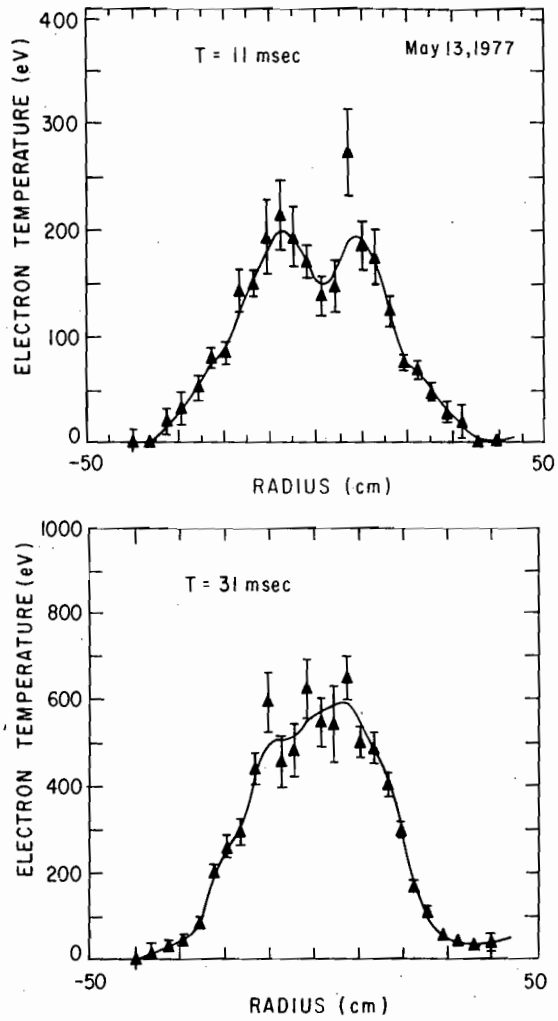

Fig. 3. Thomson scattering measurements of the electron temperature profile for the discharge shown in Fig. 2. (Courtesy of D. Johnson, PPPL).

In Fig. 2, the plasma current and loop voltage is shown for the startup phase of a high density He discharge in PLT with tungsten limiters. In addition in Fig. 3, Thomson scattering measurements of the electron temperature profile are shown. These discharges were conducted after extensive Taylor discharge cleaning. Thus, the low-Z impurity concentration was small and the inferred spectroscopic Z_{eff} was 2.1 during the startup phase. For comparison, the calculations of the one dimensional magnetic field diffusion code are shown in

Fig. 4. In this case a significant enhancement in the inferred Z_{eff} is observed. This approach has been applied to three other discharges. In two of those discharges, the maximum calculated Z_{eff} was even greater. However, in one case in which the electron temperature was low and thus the neoclassical resistivity was relatively high, the calculated and measured Z_{eff} was within experimental error.

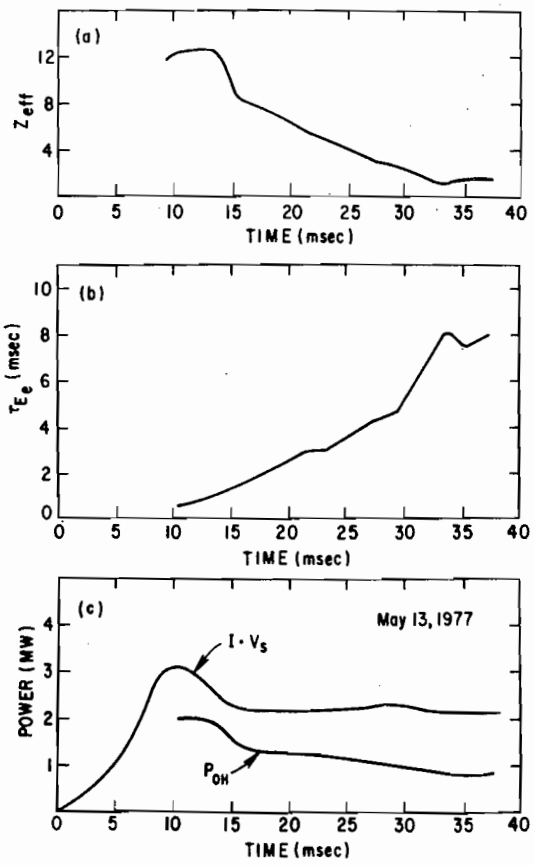

Fig. 4. The results of the calculation of Z_{eff}, τ_{Ee} and the ohmic input power from the one dimensional magnetic field diffusion code are shown.

In general, the use of a one dimensional magnetic field penetration code assuming neoclassical conductivity does not adequately model the current penetration during the startup phase of PLT. This was also found on the ST tokamak where an enhancement in the current penetration mechansim was also deduced (Hosea, 1974). So far, the mechanism responsible for the enhanced current penetration on PLT has not been identified.

In addition to the enhancement of the current penetration, this analysis indicates that the energy confinement time during the startup phase is much less than during the quasi-steady state. This may be due in part to the increased radiation losses during the startup phase. However, an enhancement in the transport process can not be excluded. Once again, these results are similar to those on the ST tokamak which also showed a shorter energy confinement time during the startup phase (Dimock and coworkers, 1973).

Plasma Conductivity During the Quasi-Steady State

The plasma conductivity in the quasi-steady state is important in determining the ohmic input power which in turn is important in the electron energy balance. Figure 5 shows the Thomson scattering measurements of the electron density and temperature throughout the high density He discharge discussed above. The one dimensional magnetic field diffusion code is used here to calculate Z_{eff} throughout the discharge including the quasi-steady state. The results of the calculation of Z_{eff} and the electron energy confinement time are shown in Fig. 6. As the density increased during the discharge, Z_{eff} decreased and frequently was less than two. In high density gettered hydrogen or deuterium discharges, Z_{eff} less than one has also been observed. (Bol and coworkers 1978; Hawryluk and coworkers 1979). So far, no satisfactory explanation has been proposed to explain this result. In these high density discharges the concentration of runaway electrons was very small and thus would not significantly modify the resistivity. It is difficult to discount the possibility of some unknown systematic error in the analysis or the measurements. Bootstrap currents which would contribute $\lesssim 5\%$ to the total plasma current have been ignored in the analysis. The error due to the analytic approximation of the neoclassical resistivity is $\sim 5\%$ and this error would tend to overestimate Z_{eff}. Z_{eff} has also been calculated without the neoclassical corrections to the plasma conductivity. In this case, Z_{eff} is typically ~ 2 in the He discharge and ~ 1 in the high density H or D discharges.

In general, during the quasi-steady state the plasma conductivity is consistent with predicted neoclassical conductivity to within a factor of 2. However, the corrections due to neoclassical effects which are typically less than a factor of 2 for present PLT operation have not yet been demonstrated conclusively. In addition, the role of MHD effects such as internal disruptions in modifying the plasma conductivity has not been clearly established. By accurately measuring the current density profile (or the q profile) in a discharge with a very low concentration of impurities, it should be possible to resolve this question. Experiments on PDX are planned to investigate this by using a diagnostic neutral beam similar to that used on ATC (Goldston 1978).

The uncertainty in the plasma conductivity affects the calculations j(r), q(r) and the ohmic input power,

$$P_{OH}(r) = j^2(r)/\sigma(r) \quad . \qquad (3)$$

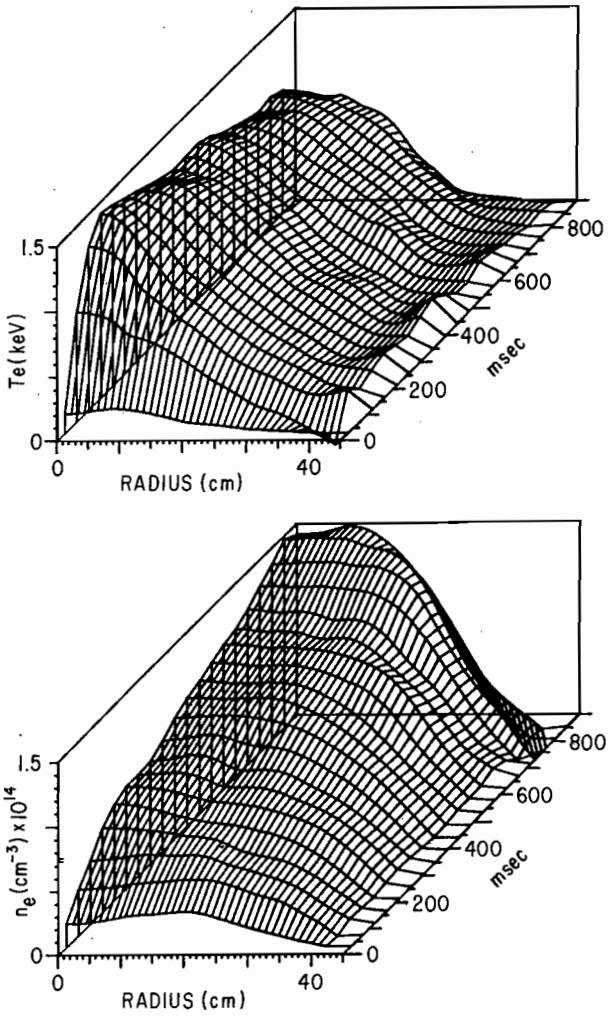

Fig. 5. Thomson scattering measurements of the electron temperature profile for the discharge shown in Fig. 2 and 3. (Courtesy of D. Johnson, PPPL).

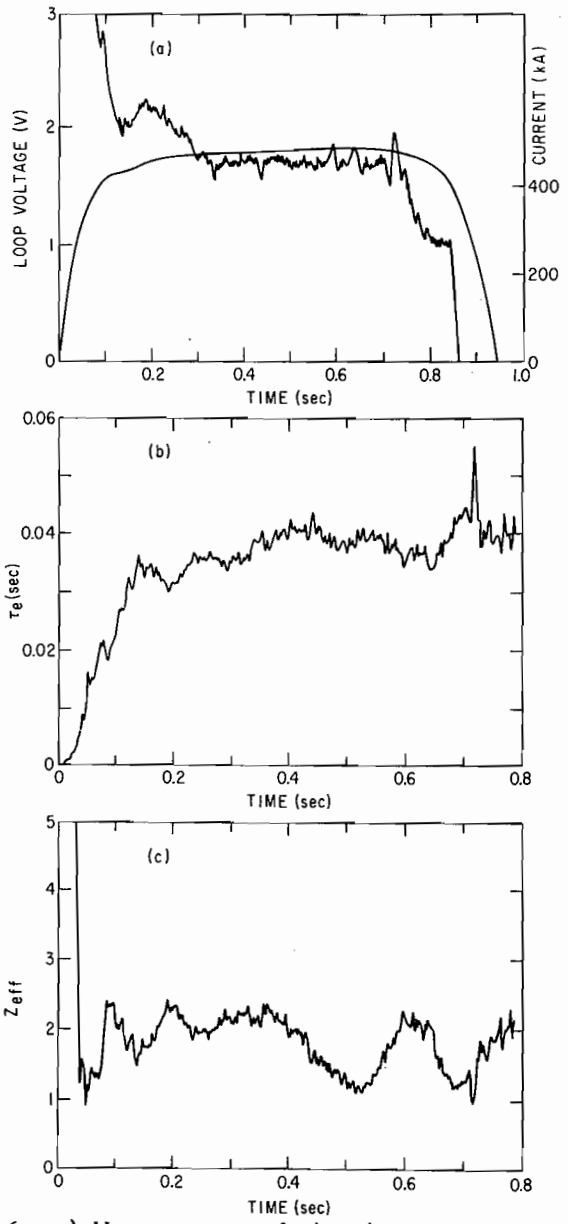

Fig. 6. a) Measurements of the plasma current and the loop voltage are shown for the discharge shown in Fig. 5. b) and c) Calculations of the electron energy confinement time and Z_{eff} respectively from an analysis of the one dimensional magnetic field diffusion.

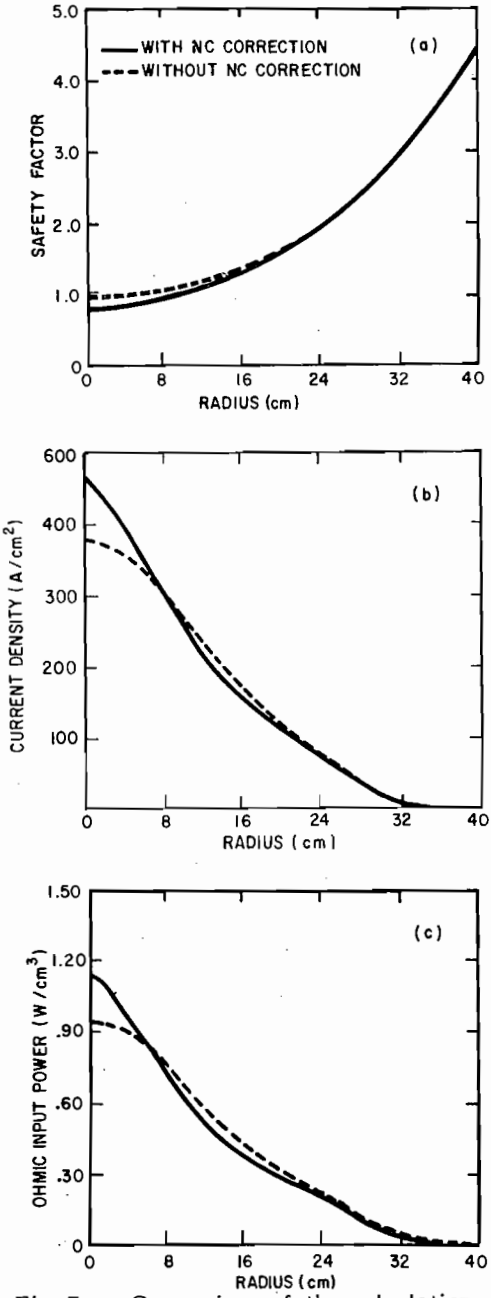

Fig. 7. Comparison of the calculation of the safety factor, the current density and the ohmic input power with and without the neoclassical correction to the plasma conductivity for the discharge shown in Fig. 5 at 630 msec.

Figure 7 illustrates this by comparing the results of the calculation with and without the neoclassical corrections for the high density He discharge shown in Fig. 5. The effect of the neoclassical correction is to decrease the conductivity in the middle region of the discharge and thus to increase the current density on axis. In some high density hydrogen or deuterium discharges, the effect can be somewhat greater. The resulting uncertainty of 20-30% in the local ohmic input power in the core of the discharge, though not very large, results in a somewhat greater uncertainty in the electron heat conductivity in the core of the discharge.

CONSERVATION OF PARTICLES[2]

The particle conservation equation is

$$\frac{\partial n}{\partial t} = - \frac{1}{r}\frac{\partial}{\partial r} (rnV) + S \quad , \tag{4}$$

where n is the local particle density, V is the radial flow velocity and S is the local source function. In the analysis code, the particle conservation equation for the background plasma (two species), one impurity species and the electrons are considered in addition to the beam ions. In this lecture, only the background plasma ions and electrons will be considered. The evolution of the high density He discharge in which $n_e(0)$ increases to $\sim 1.5 \times 10^{14}$ cm^{-3} (see Fig. 5) will be analyzed to determine the radial flow velocity which can be obtained by integrating Eq. 4:

$$V(r) = \frac{1}{rn} \int_0^r \left(S - \frac{\partial n}{\partial t} \right) r' dr' \quad . \tag{5}$$

The rate of change of density is determined from the experimental measurements whereas the local source function is calculated on the basis of a neutral penetration model.

Neutral Penetration Model

Neutral density within the discharge core provides a local ionization source. In the absence of significant recombination, penetration by repeated charge exchange collisions is the process by which the neutral density profile is established. The dominant charge exchange reaction is that between Helium neutrals and He^{++}. Because of its size, substantial attenuation of the flux of charge exchange neutrals can occur in the PLT device at the moderate electron densities reached in helium discharges. A Monte Carlo technique has been used to calculate this attenuation (Hughes and Post, 1978).

Two separate neutral fluxes are modeled in calculating the neutral density – a flux of cold neutrals corresponding to those introduced directly by gas injection, and a flux of warm neutrals, corresponding to particles recycling at the limiter. An average neutral energy of 30 to 40 eV is observed throughout the density rise by Doppler broadening measurements of neutral helium. A Maxwellian velocity distribution with this average energy is therefore assumed for the warm neutrals at the plasma boundary in this calculation. In an effort to obtain an upper limit on the helium neutral density within the core of the discharge, all neutrals escaping from the plasma volume are assumed to reflect at the wall with no loss of energy.

The absolute magnitude of the neutral density is determined by a normalization of the Monte Carlo results. The Monte Carlo procedure in conjunction with Thomson scattering profiles of

[2]The analysis of the high density He discharge presented here is a summary of the work by G. L. Schmidt, N. Bretz, M. Hughes, R. J. Hawryluk, D. W. Johnson and J. A. Schmidt (1977).

density and temperature, is used to calculate the radial dependence of the neutral density, f(r). The volume integral of the source function associated with f(r) is then computed. In the case of cold neutrals, this integral is normalized to the measured increase in the particle content of the discharge. In the case of warm neutrals, the integral is normalized to the measured particle replacement losses. (This approach implicitly assumes that the recycling coefficient is unity.) Azimuthal asymmetries during the density rise, limit the accuracy with which particle replacement losses are known for the discharges considered here. Measurements at a single location indicate that replacement times are less than 10 ms and nearly constant in time. An average value of 10 ms is more consistent with the energy input to the discharge and this value is used here. Note that this value of the particle replacement time is significantly less than the discharge energy confinement time, indicating that strong recycling of low temperature edge plasma occurs during density build up. Such recycling leads to enhanced levels of neutral density throughout the discharge. Since the recycling flux dominates the problem, the neutral density and the electron source scales linearly with replacement time.

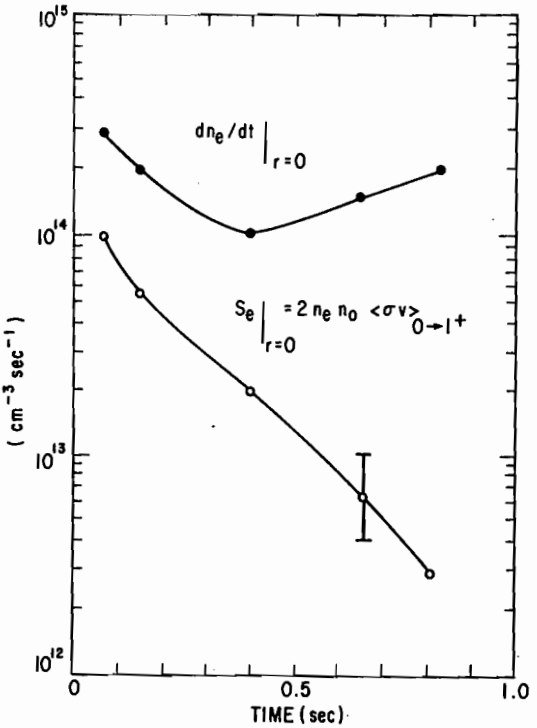

Fig. 8. Comparison of the calculated electron source on axis with the observed rate of rise of the electron density.

Figure 8 compares the calculated electron source term on axis due to ionization of neutral helium with the measured change in central density during the discharge. The source term is decreased to a value more than an order of magnitude less than the observed rate of density increase, and cannot alone account for the observed rate.

Ionization of low-Z impurities (principally oxygen) does provide an additional electron source term. However, in these discharges the concentration of oxygen is low. Estimates of the source function associated with this flux indicate that its magnitude is comparable to the He source function within the core of the discharge and thus insufficient to account for the observed density rise.

Radial Flow Velocity

On the basis of the calculated electron source function and the observed density rise, the flow velocity was calculated using Eq. 5 as shown in Fig. 9. To account for the density rise on axis, the flow velocity in the core of discharge is inward though small in magnitude. In the plasma periphery, it is outward and its magnitude is clearly much larger.

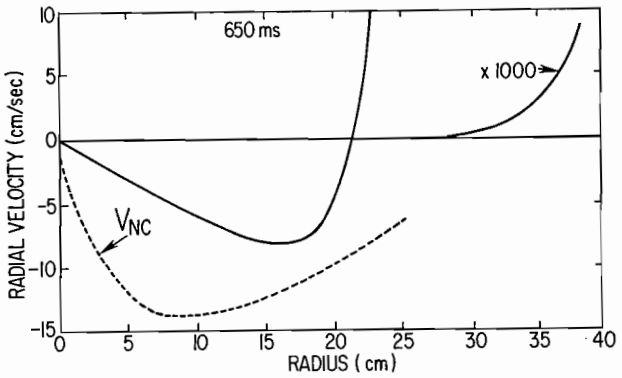

Fig. 9. Comparison of the inferred radial flow velocity with the predicted neoclassical pinch at 650 msec into the discharge.

For comparison, the neoclassical pinch velocity was calculated using the results of Hirshman and Sigmar (1977) and also Hirshman (1978) as shown in Fig. 9. The neoclassical pinch, possibly with some small enhancement ($\lesssim 2$), could provide the required inward flow in the PLT discharges studied to date. However, the radial variation of the pinch and the deduced flow velocity are significantly different. To account for the difference, it is necessary to assume an additional anomalous outward flux in addition to the pinch velocity. For simplicity if the outward flux is assumed to be proportional to ∇n, then

$$D \frac{\partial n_e}{\partial r} = n_e \left(V(r) - V_{NC}(r) \right), \qquad (6)$$

and the anomalous radial particle diffusion coefficient, D, can be obtained because the right hand side is known. The results of this calculation are shown in Fig. 10. The anomalous

transport coefficients both in the interior and exterior of the discharge are much larger than predicted by neoclassical theory. This anomalous particle diffusion coefficient is required to account for the radial profile and the large recycling at the edge. It should be kept in mind, however, that this model is not unique. For instance the anomalous particle flux can be a combination of both inward and outward fluxes and not necessarily simply proportional to the electron density gradient. Thus, the role of the neoclassical pinch in the density buildup has not been established.

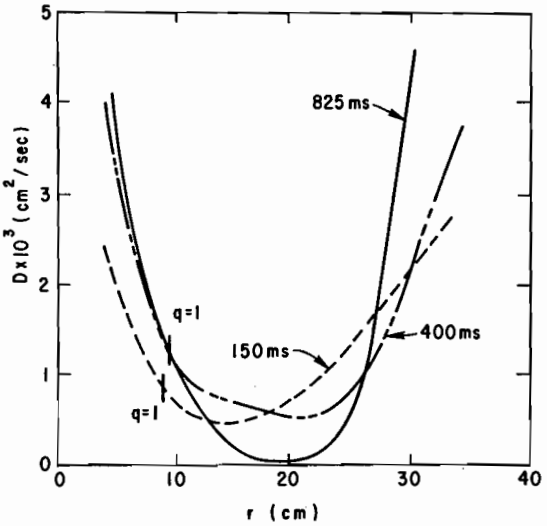

Fig. 10 Calculation of the anomalous particle diffusion coefficient assuming that the inward flux is due solely to the neoclassical pinch and that the outward flux is proportional to ∇n_e.

ELECTRON AND ION ENERGY BALANCE

General Considerations

The energy balance equation derived by Braginskii (1965) can be expressed as:

$$\frac{3}{2}\frac{\partial}{\partial t} nT \quad + \nabla \cdot \frac{5}{2} nT\vec{V} \quad - \vec{V} \cdot \nabla nT \quad + \pi_{\alpha\beta}\frac{\partial V\alpha}{\partial x_\beta} + \nabla \cdot \vec{q} = Q \quad . \quad (7)$$

The first term is the rate of change of thermal energy. The following three terms are related to particle fluxes where $\pi_{\alpha\beta}$ is the stress tensor. The fourth term is the heat flux and represents the transport of energy associated with the random motion in the coordinate system in which the particle flow velocity is zero. The last term is the heat generated by collisions between two different species. Because of the choice of the coordinate system in which Q is defined,

$$Q_e = - Q_i - \vec{R}_{ei} \cdot (\vec{V}_e - \vec{V}_i) \qquad (8)$$

where $\vec{R}_{ei}$ is the change of momentum due to collisions between electrons and ions. The term on the left hand side corresponds to both the force of friction due to the existences of a relative velocity (ohmic heating) and a thermal force which, in a simple classical plasma, arises from the presence of a temperature gradient.

As a consequence of the kinetic equations or of a particular microinstability model, it is possible to calculate $\vec{V}$, $\pi_{\alpha\beta}$, $\vec{q}$, and Q. In general, this is not the approach most commonly used in either one dimensional transport code or in analysis codes such as the one being described to analyze experimental data. Rather, Eq. 7 is substantially simplified. The usual approximations are:

(1) Consider variations only in the radial direction (1-D approximation).
(2) Neglect the stress tensor.
(3) Assume that the coupling between the ions and the electrons is due to Coulomb collisions, ($Q_i = q_{ie}$ due to Coulomb collisions).
(4) Include charge exchange loss, neutral heating, ionization losses and impurity radiation.
(5) Set $q_r = \kappa n \partial T/\partial r$ where κ is the heat conductivity due either to neoclassical heat conduction or anomalous processes.

At this point, there is a divergence of opinion as to what the convective power loss is. In order to understand where the disagreement comes from, the frictional momentum force, R_{ei}, must be calculated (Goldston, 1979). From the conservation of momentum equation,

$$\vec{R}_{ei} \cdot (\vec{V}_e - \vec{V}_i) = p_{OH} + \vec{V}_e \cdot \nabla p_e + \vec{V}_i \cdot \nabla p_i, \qquad (9)$$

neglecting the stress tensor and terms of $O(V^2)$. Substitute Eqs. (8), and (9) into Eq. (7) and quantitatively identify the terms originating from convection as being related to the radial flow velocity, then

$$p^i_{conv} = \nabla \cdot \left(\frac{5}{2} n_i T_i \vec{V}_i\right) - \vec{V}_i \cdot \nabla p_i \qquad (10)$$

and

$$p^e_{conv} = \nabla \cdot \left(\frac{5}{2} n_e T_e \vec{V}_e\right) + \vec{V}_i \cdot \nabla p_i \quad . \qquad (11)$$

The last term on the right hand side can be considered to be the dissipation of the induced drifts due to radial diffusion. Note that in a classical plasma, the ion drifts are dissipated by electron-ion collisions. This results in a transfer of power from the ions to the electrons. This simple concept carries over into neoclassical theory, although the resulting equations are somewhat more complex. However, the particle fluxes in a tokamak are not a result of only Coulomb collisions since the observed radial velocity does not agree with the predictions of neoclassical theory. Thus, the way these fluxes are dissipated is dependent upon the theoretical model proposed to explain the fluxes. This accounts in part for the difference in the various computational simulations where the conduction loss is given by the Braginskii equation or by

$$\nabla \cdot \left(\frac{5}{2} nT\vec{V}\right) \quad \text{(Stott, 1976)} \qquad (12)$$

or

$$\nabla \cdot \left(\frac{3}{2} nT\vec{V}\right) \quad \text{(Düchs, Post and Rutherford 1977).} \qquad (13)$$

Until now Eqs. (10) and (11) have been used in the transport analysis code. However, without a priori, knowing what the kinetics of the radial transport mechanism are it is difficult to determine which approximation is more accurate. The differences between these approximations are not negligible since they introduce about a factor of two uncertainty in the power loss due to convection.

Thus, the following equations have been used in the transport analysis code for the electron and ion energy balance:

$$\frac{3}{2}\frac{\partial}{\partial t} n_e T_e + \frac{1}{r}\frac{\partial}{\partial r}\left(\frac{5}{2} r n_e T_e V_e\right) + \sum_k V_k \frac{\partial}{\partial r} n_k T_i$$

$$- \frac{1}{r}\frac{\partial}{\partial r} r n_e \kappa_e \frac{\partial}{\partial r} T_e = P_{OH} - q_{ie} - P_{ioniz} - P_{rad} \qquad (14)$$

and

$$\frac{3}{2}\frac{\partial}{\partial t} n_i T_i + \sum_k \left[\frac{1}{r}\frac{\partial}{\partial r}\left(\frac{5}{2} r n_k T_i V_k\right) - V_k \frac{\partial}{\partial r} n_k T_i\right.$$

$$\left. - \frac{1}{r}\frac{\partial}{\partial r} r n_i \kappa_i \frac{\partial}{\partial r} T_i = q_{ie} - P_{chx} + P_{neut} \right. . \qquad (15)$$

The power loss by ionization is given by

$$P_{ioniz} = n_e n_o \langle \sigma v \rangle_{ioniz} W_{ion} \ , \qquad (16)$$

neglecting the power loss by impurity ionization. However, the power radiated by impurities, P_{rad} is accounted for. The radiated power is obtained from bolometric measurements of the total power to the wall, which includes both charge exchange and radiation. Assuming that the power is predominantly due to radiation, the bolometer measurements are Abel inverted to give the local radiated power. If the flux were mainly charge exchange, then the validity of the inversion would be uncertain (Hsuan and coworkers, 1978).

In the electron and ion energy balance, the summation over k includes all of the hydrogenic and impurity ions and the total ion density is denoted by n_i. The power loss by charge exchange between a hydrogenic ion, n_H, and a neutral is given by

$$P_{chx} = \frac{3}{2} n_H n_o \langle \sigma v \rangle_{chx} (T_i - T_o) \ , \qquad (17)$$

where the neutral density, n_o and neutral temperature, T_o, are determined by the neutral penetration code. The power gained by ionizing a hot neutral is

$$P_{neut} = \frac{3}{2} n_e n_o \langle \sigma v \rangle_{ioniz} T_o \qquad (18).$$

As mentioned above when this code is used to analyze experimental data, the ion temperature profile is calculated and compared with experimental measurements. As a working hypothesis, the ion heat conductivity, κ_i, is assumed to be given by neoclassical transport theory $\kappa_i = \alpha \kappa_i^{NC}$. In order to evaluate this hypothesis, the factor, α, is varied. In my other lecture, a summary of the experimental results pertaining to the ion energy balance is presented. The neoclassical ion heat conductivity is calculated using the results of Rutherford

and coworkers (1976). For $Z_{eff} = 1$ plasma, this formulation agrees with that of Hazeltine and Hinton (1976) in the banana region of neoclassical theory ($\nu_{*H} = 0$). However, in the transition regime between the plateau and banana regime ($\nu_{*H} = 1$), the calculation of Rutherford and coworkers (1976), are a factor of ~1.7 greater than that of Hazeltine and Hinton (1976). Accurate analytic approximations for the conductivity corresponding to a multi-specie plasma (H, D, impurity and beam ions) for different collisionality parameters (banana, plateau and Pfirsch-Schlüter) would be very useful. Though it is difficult to infer the ion heat conduction to within a factor of two experimentally, theoretically at least it should be known more accurately than that. This is important in obtaining a better estimate of the agreement between the inferred ion heat conduction and the predictions of neoclassical theory.

In the remainder of this lecture, a high and a low density ohmically heated discharge will be analyzed to illustrate the important terms in the ion and electron energy balance. In the workshop, Dr. Goldston includes the deposition of power and particles due to neutral beam injection, in using this approach to analyze the neutral beam heating experiments on PLT.

High Density Discharge

The first discharge which will be considered is a high density deuterium discharge with stainless steel limiters. In these discharges, the conductivity Z_{eff} was ~1 in the quasi-steady state assuming neoclassical conductivity. In Fig. 11, the density and temperature profiles are shown at 500 msec into the discharge while the density was still rising. Assuming $\kappa_i = \kappa_i^{NC}$ and $\tau_p = 30$ msec, the ion energy balance is calculated. (In both this case and the next, the particle confinement time was not measured and it is treated as a free parameter.) In Fig. 12, the volume integrated power flow and loss terms are calculated. For instance, the net charge exchange loss within a radius r is

$$P_{chx} = 4\pi^2 R \int_o^r P_{chx}\, r dr \quad .$$

This uncertainty in τ_p does not affect the central ion temperature in high density discharge, but it does not affect the power loss by convection in the plasma periphery. A short τ_p increases ion convection and thus power flow from the electrons to the ions. If τ_p is too short for instance < 10 msec, then the results for the electron energy balance are not consistent, as will be discussed further.

The effect of varying the ion neoclassical heat conductivity is shown in Fig. 13. A factor of 3 variation results in only ~10% variation in the central ion temperature. Because the electrons and ions are well equilibrated, the ion temperature is almost proportional to the electron temperature. Thus, to detect the effect of anomalous ion heat conduction both the error in the electron and ion temperature must be less than 3%. This is very difficult to achieve.

While it is very difficult to determine the electron-ion heat transfer in high density discharges because of the required accuracy in both the electron and ion temperature measurement, it is possible to obtain an upper limit. The maximum power that can go from the electrons to ions and thus be transport through the ion channel is the ohmic input power. Thus in the discharge in Fig. 10, the maximum permissible enhancement in the neoclassical ion heat transport is a factor of 5. In somewhat higher density deuterium discharges, the maximum enhancement in the neoclassical heat-conduction is a factor of 2-3. In contrast in high density discharges in Alcator A, it was observed that neoclassical ion heat transport could account for the heat transport in the core of the discharge (Gondhalekar and coworkers, 1978).

The electron energy balance for the high density discharge is shown in Fig. 14. In the core of the discharge ($r < 20$ cm), 60% of the power is lost by electron heat conduction. The

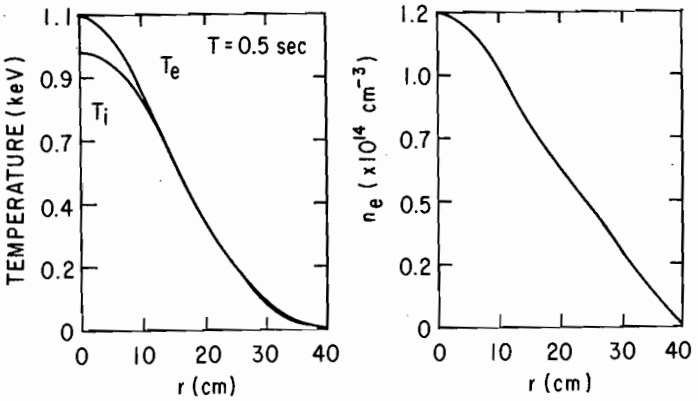

Fig. 11. Thomson scattering measurements of the electron temperature and density profile and the calculated ion temperature profile for a high density deuterium discharge with stainless steel limiters. (Courtesy of D. Johnson, PPPL).

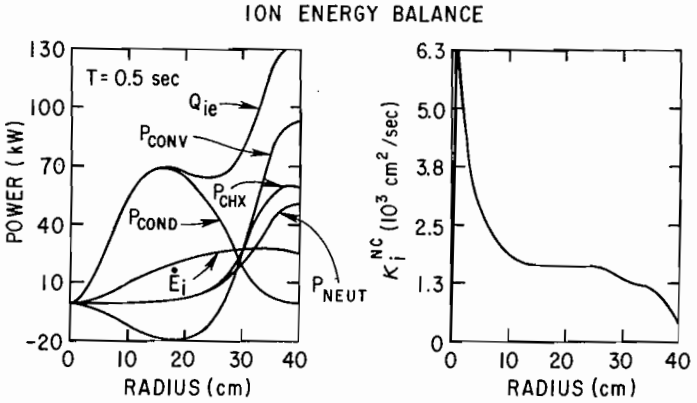

Fig. 12. The ion energy balance for the discharge shown in Fig. 11. The volume integrated power and the neoclassical ion heat conductivity as a function of radius are shown.

remaining power is lost mainly by radiation (22%) and electron-ion coupling (15%). Near the axis of the discharge, electron-ion coupling accounts for a somewhat larger fraction of the power input (~25%) and the electron heat conductivity is only a factor of ~1.7 larger than the ion. However, the electron heat conductivity has a spatial variation which is considerably different than the ion neoclassical heat conductivity (see Figs. 12 and 14). The electron heat conductivity tends to increase with minor radius. This is a fairly general result, though in some discharges the radial variation is less pronounced.

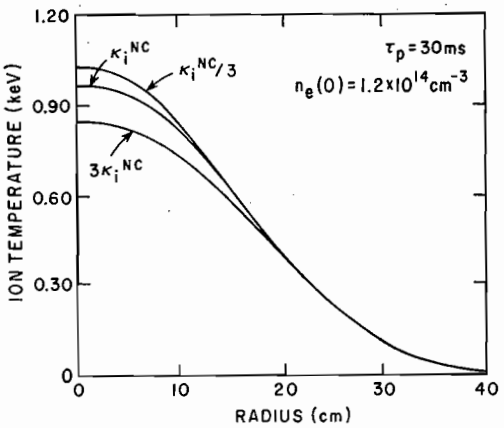

Fig. 13. Illustrates the effect on the ion temperature profile by varying the neoclassical ion heat conductivity by a factor of 3.

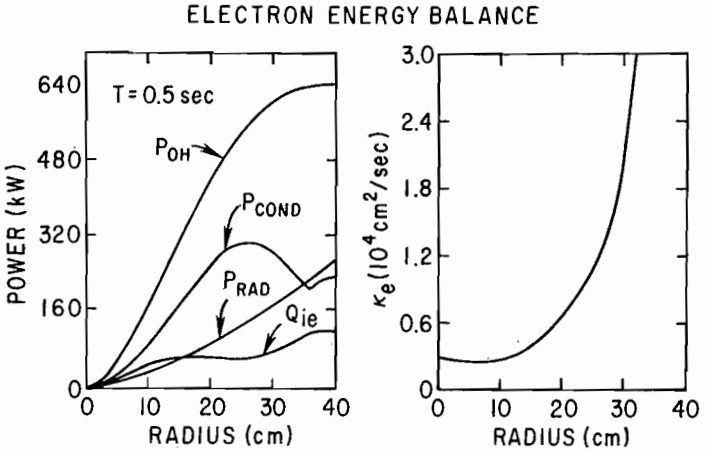

Fig. 14. The electron energy balance for the discharge shown in Fig. 11. The volume integrated power and the inferred electron heat conductivity as a function of radius are shown.

There are several sources of error in the calculation of κ_e. The first is the evaluation of the electron temperature gradient. Depending upon the accuracy of the data the uncertainty in evaluating the temperature gradient can be significant. While in this discharge the profile was relatively well known, they are not always, as will be shown in the low density discharge. The

second, is the model for the plasma resistivity. In these calculations, neoclassical resistivity was assumed. If Spitzer resistivity were used, then the electron heat conductivity would decrease within the inner 10 cm by 60% and the fraction of power going through the ion channel would increase to 30% in the region. Outside of the inner 10 cm, the difference between neoclassical and Spitzer resistivity is minimal. The third is the uncertainty in the particle confinement time. This has a small effect except near the plasma periphery ($r > 30$ cm). If τ_p is assumed to be too small then the power loss by convection can be greater than the ohmic input power minus the power loss by radiation and ionization. This is useful in determining the minimum τ_p consistent with the density and temperature profiles. The fourth uncertainty is due to the measurements of the bolometric power. Depending upon the toroidal location of the bolometer, charge exchange may contribute significantly to the power flux which the bolometer measures. This must be considered in interpreting the validity of the calculation. In general while a transport analysis code appears to be useful in determining κ_e in the interior of the discharge, the results in the plasma periphery ($r > 30$) are very suspect, due to the uncertainties in τ_p, power radiated and to a lesser extent the accuracy of the density and temperature profiles. Similar problems are encountered by one dimensional simulation codes in the plasma periphery where adhoc prescriptions limiting the heat conduction and particle transport are often employed.

Low Density Discharge

The electron temperature and density profiles for a low density hydrogen discharge which was used as the target plasma for neutral beam injection are shown in Fig. 15. In this case, water cooled graphite limiters were used and the conductivity Z_{eff} was ~ 2.5, again assuming neoclassical conductivity. Unlike the preceeding case, the electron temperature gradient is strongly varying with minor radius. Whether these variations are meaningful is not certain. The uncertainty in the electron temperature gradient is manifest in the calculation of the electron heat conductivity. In this discharge, the central ion temperature was in the range of 800-1000 eV.

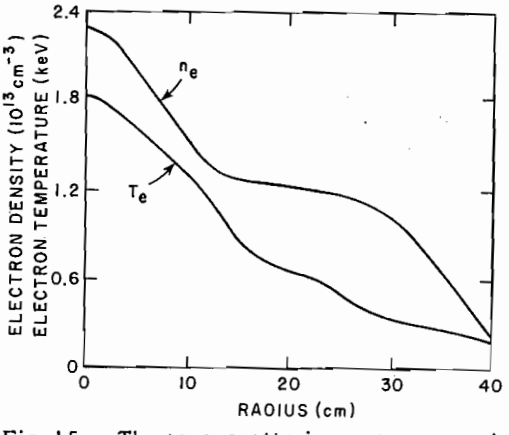

Fig. 15. Thomson scattering measurements of the electron density and temperature profile for a low density hydrogen discharge. (Courtesy of D. Johnson, PPPL).

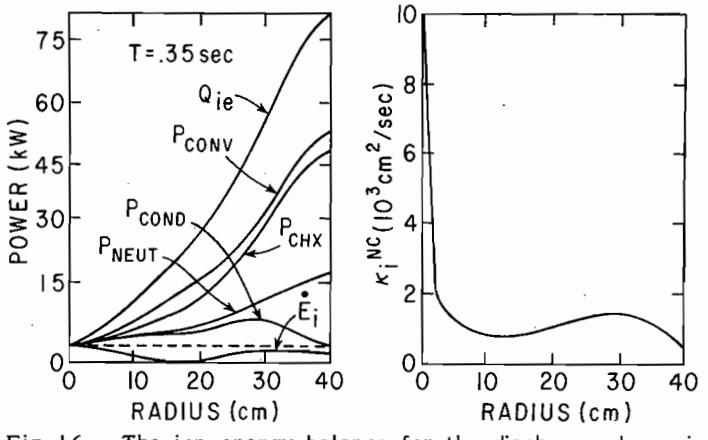

Fig. 16. The ion energy balance for the discharge shown in Fig. 15. The volume integrated power and the neoclassical ion heat conductivity as a function of radius are shown.

The ion energy balance is presented in Fig. 16, assuming $\kappa_i = \kappa_i^{NC}$ and τ_p = 30 msec. In this discharge, the ion energy balance in the core is dominated by particle convection and charge exchange loss with neoclassical heat conduction being relatively unimportant. These results are sensitive to the uncertainty in the neutral density profile which is illustrated by varying τ_p (which was not measured) as shown in Fig. 17. The central neutral density must be known to better than a factor of three so that the uncertainty in the neutral density is not important in the analysis of the heat conduction. The effect of varying the ion heat conduction coefficient can be seen in Fig. 18 assuming τ_p = 30 msec. If τ_p were 30 msec, then the maximum possible enhancement in κ_i is about a factor of 3. However, if τ_p = 100 msec, then the maximum permissible enhancement is about a factor of 7. For this low density discharge, the total electron-ion heat transfer as well as the heat which is transported by conduction and convection is considerably larger than the power loss by ion neoclassical heat transport. Even if the ion heat conductivity were adequately predicted neoclassical theory, then particle convection still remains a significant source of anomalous heat transport at low densities. Clearly an understanding of the anomalous particle transport mechanism and how it scales in necessary in low density discharge.

The electron energy balance assuming τ_p = 30 msec and $\kappa_i = \kappa_i^{NC}$ is shown in Fig. 19. Once again, electron heat conduction dominates the power balance in the interior of the discharge. However, now the electron-ion coupling is a very small part ($\lesssim$10%) of the total electron power balance. In the low density discharge, the electron heat conductivity is considerably larger than in the high density discharge reflecting the decreased electron density. The large radial variations in κ_e are due to the variations in the electron temperature gradient. This shows the necessity for reliable data. As both measurement of soft x-ray emission and computational simulation of islands due to tearing modes indicate, that the electron temperature profile could, in principle, be substantially altered. However, in this case, the variation in the electron temperature gradients are not beyond experimental error. Thus, the large radial variation in κ_e shown in Fig. 19 may be an artifact.

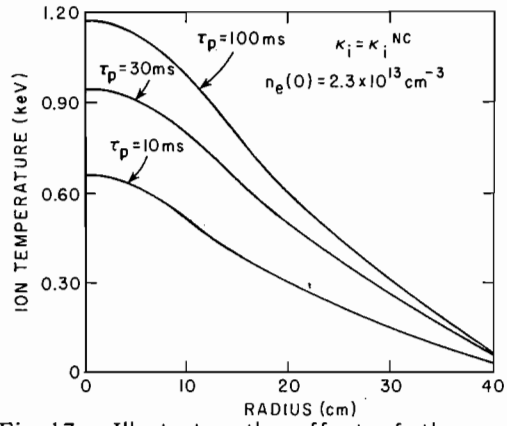

Fig. 17. Illustrates the effect of the uncertainty of the particle confinement time and, hence, the neutral density profile on the calculated ion temperature profile.

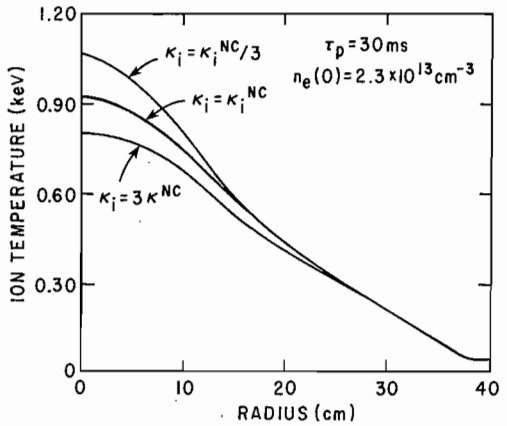

Fig. 18 Illustrates the effect on the ion temperature profile by varying the neoclassical ion heat conductivity by a factor of 3.

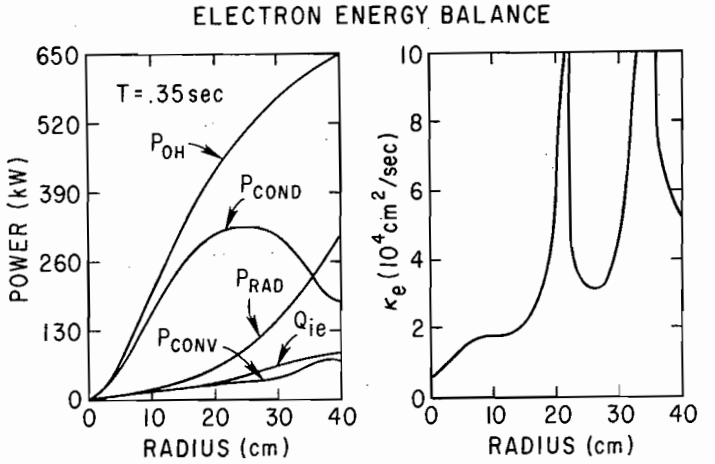

Fig. 19. The electron energy balance for the discharge shown in Fig. 15. The volume integrated power and the inferred electron heat conductivity as a function of radius are shown.

CONCLUDING REMARKS

The transport analysis code is useful in interpreting experimental measurements and facilitates an understanding of transport phenomenon in a tokamak discharge. In addition, one of the results of the transport analysis code has been an insight into the remaining unanswered questions and the diagnostic measurements required to provide an answer. This final section will review the principal problems which remain to be solved.

The analysis of the evolution of the poloidal magnetic field indicates the importance of direct measurements of the current density or the safety factor profile. This is necessary in the startup phase in order to evaluate the effect of MHD instabilities on the evolution of the poloidal magnetic field directly. In the quasi-steady these measurements are necessary in order to verify the model for the plasma conductivity and determine whether the predicted bootstrap currents are present. In addition, it would be useful to evaluate changes in the current density profile due to beam or rf induced currents or MHD effects associated with rapid plasma heating to high β configurations.

In order to improve our understanding of both the radial flux of particles as well as the ion energy balance in low density discharges especially during neutral beam injection, measurements of the flux surface averaged neutral density profile are required. These measurements would also be useful in verifying the neutral penetration models. However because of the large radial, poloidal, and toroidal variations in the neutral density profile, accurate measurements are very difficult.

The analysis of the particle transport in high density discharges demonstrates the presence of an inward flux of particles in addition to the large outward flux in the periphery. The fundamental question is not the magnitude of the fluxes but whether these fluxes simply results from the inward, though perhaps enhanced, pinch in addition to an outward flux proportional to the electron density gradient (Hughes 1978; Schmidt and coworkers, 1977). For instance, are the fluxes related to the electron temperature gradient as predicted by Coppi and Spight, (1978) and Antonsen, Coppi and Englade (1979) ?

One indication that particle transport may be considerably more complicated and difficult to understand is the observation on PLT of large poloidal asymmetries in the low ionization states of oxygen and carbon in the plasma periphery (Suckewer, Hinnov, and Schivell, 1978). Unlike similar observation on Alcator (Terry and coworkers, 1977) these do not correlate with ∇B drifts.

The analysis of the ion energy blance in low density discharges indicates that the power loss by convection as well as by neutral loss can be significant. Low density discharges in conjunction with neutral beam heating has resulted in high ion temperatures in PLT (Eubank and coworkers, 1978; 1979). This "hot ion mode" may be attractive in future experiments operating more closely to ignition (see Dr. Clarke's lecture). Under these conditions a better understanding of particle transport and the corresponding power loss by convection will be especially important. In addition to the uncertainty in convection, the uncertainty in the ion power loss by conduction and the possible role of anomalous ion heat conduction must be considered in extrapolating to future experiments. In low density discharges, the uncertainty of the validity of the ion neoclassical theory prediction of the ion heat conduction is at least a factor of 2-3 in ohmically heated discharges and somewhat greater in neutral beam injection discharges. Due to the uncertainty in both the measurements and the interpretation, it is difficult to conclude that the ion heat conduction agrees with neoclassical theory predictions by much better than a factor of two under all conditions of interest. However, it is possible under some special cases such as high density discharges to more accurately verify the prediction of the neoclassical theory. Nonetheless, it is difficult to exclude in general the presence of anomalous ion heat conduction comparable with neoclassical ion heat conduction.

Perhaps one of the most fundamental questions associated with the analysis of both the electron and ion power balance is the validity of the assumption that the electron-ion coupling is due to Coulomb collisions. Unfortunately, it is very difficult to verify this assumption in a tokamak discharge. On the basis of their analysis of the ion temperature balance in TFR-400, Equipe TFR (1978) concluded that both enhanced ion heat transport and electron-ion coupling may be required to explain the ion energy balance depending upon ones faith in the accuracy of the profile measurement in the plasma periphery. In addition, in the low density slide-away regimes in the Alcator discharge, enhanced ion heating was observed (Oomens and coworkers, 1976). Both of these results suggest that a greater effort should be made to determine how well the power which is transferred from the electrons to the ions is predicted by Coulomb collisions. One observation which supports this model is that the slowing down spectrum of neutral beam injected neutrals is well described by classical processes (see Dr. Goldston's lecture). In addition, an upper limit on the electron-ion coupling is the ohmic input power. This places fairly stringent constraints on high density discharges though not on low density discharges (see Fig. 19.).

Electron heat conduction is the dominant power loss in the core of the discharge except in high density discharges where ion neoclassical heat transport is important and in radiation dominated discharges. So far, it has been difficult to establish the parametric dependence of the electron heat conductivity conclusively. This is in part due to our limitations in inferring the conductivity from the experimental measurements. In addition, it is difficult to vary plasma parameters independently (except perhaps for the electron density) in order to evaluate the implication of different hypothesis. This is an especially important limitation in ohmically heated discharges in which the heat conductivity, current density and temperature are strongly coupled. As a result of supplementary heating it should be possible to vary the temperature and the current density independently. For instance in PLT, the electron heat conductivity during neutral beam injection was observed to decrease in the plasma core (Eubank and coworkers 1978; 1979). While these results are interesting many more discharges conducted under a wide range of parameters will have to be analyzed before it will be possible to determine the parametric dependence of the electron heat conductivity. In the next few years with the application of intense auxiliary heating and the development of accurate diagnostics, it should be possible to make substantial progress in understanding cross-field transport.

REFERENCES

Antonsen, T., B. Coppi, R. Englade (1979). Inward Particle Transport by Plasma Collective Modes. Nucl. Fusion 19, 641-658.

Bol, K., et al. (1978). Radiation, Impurity Effects, Instability Characteristics and Transport in Ohmically Heated Plasmas in the PLT Tokamak. In Plasma Physics and Controlled Nuclear Fusion Research (Proc. 7th Int. Conf. Innsbruck, 1978) 1, IAEA, Vienna (1979) pp. 11-32.

Braginskii, S. I. (1965). Transport Processes in Plasmas. In Reviews of Plasma Physics, edited by M. A. Leontovich (Consultants Bureau, New York) Vol. 9. pp. 205-309.

Bretz, N., D. Dimock, V. Foote, D. Johnson, D. Long, and E. Tolnas (1978). Multichannel Thomson Scattering Apparatus. Appl. Optics 17, 192-202.

Brusati, M., S. L. Davis, J. C. Hosea, J. D. Strachan, and S. Suckewer (1978). Ion Energy Balance in Ohmically Heated PLT Discharges. Nucl. Fusion 18, 1205-1216.

Coppi, B. and C. Spight (1978). Ion Mixing Mode and Model for Density Rise in Confined Plasmas. Phys. Rev. Letters 41, 551-554.

Dimock, D. L., H. P. Eubank, E. Hinnov, L. C. Johnson and E. B. Meservey (1973). Ontogeny of a Tokamak Discharge. Nucl. Fusion 13, 271-280.

Duchs, D. F., D. E. Post, P. H. Rutherford (1977). Computer Model of Radial Transport in Tokamaks. Nucl. Fusion 17, 565-609.

Equipe TFR (1978). High Power Neutral Injection and Ion Power Balance in TFR. Nucl. Fusion 18, 1271-1303.

Eubank, H. et al. (1978). PLT Neutral Beam Heating Results in Plasma Physics and Controlled Nuclear Fusion Research, (Proc. 7th Int. Conf. Innsbruck, 1978) 1, IAEA (1979), pp. 167-197.

Eubank, H. et al. (1979). Neutral-Beam Heating Results from the Princeton Large Torus. Phys. Rev. Letters 43, 270.

Gaudreau, M. et al. (1977). High-Density Discharges in the Alcator Tokamak. Phys. Rev. Letters 39, 1266.

Goldston, R. J. (1978). Radially Resolved Measurements of "q" on the Adiabatic Toroidal Compressor Tokamak. Phys. Fluids 21, 2346.

Goldston, R. J. (1979) private communication.

Gondhalekar, A., et al. (1978). Study of the Energy Balance in Alcator in Plasma Physics and Controlled Nuclear Fusion Research. (Prof. 7th Int. Conf. Innsbruck, 1978) 1, IAEA (1979), pp. 199-209.

Hinton, F. L. and R. D. Hazeltine (1976). Plasma Transport in Toroidal Confinement Systems. Rev. Mod. Physics 48, 239-308.

Hirshman, S. P., and D. J. Sigmar (1977). Neoclassical Transport of a Multispecies Toroidal Plasma in Various Collisonality Regimes. Phys. Fluids 20, 418-426.

Hirshman, S. P., R. J. Hawryluk, B. Birge (1977). Neoclassical Conductivity of a Tokamak Plasma. Nucl. Fusion 17, 611.

Hirshman, Steven, P. (1978). Neoclassical Curent in Toroidally-Confined Multispecies Plasma. Phys. Fluids 21, 1295-1301.

Hosea, J. C. (1974). Ohmic Heating of Tokamak. Symposium on Plasma Heating in Toroidal Devices, Varenna, Italy. Editrice Corporation pp. 189-198.

Hsuan, H. et al. (1978). Energy Balance of the PLT Tokamak. Proc. Joint Varenna and Grenoble Int. Symp. on Heating in Toroidal Plasmas, Grenoble (1978).

Hughes,M. H. (1978) Numerical Calculation of Transport in Alcator. PPPL-1411.

Hughes, M. H. and D. E. Post (1978). A Monte Carlo Algorithm for Calculating Neutral Gas Transport in Cylindrical Plasmas. J. Comp. Phys. 28, 43-55.

Oomens, A. A. M., L. Th. M. Ornstein, R. R. Parker, F. C. Schuller and R. J. Taylor (1976). Observation of High-Frequency Radiation and Anomalous Ion Heating on Low-Density Discharges in Alcator. Phys. Rev. Letters 36, 255-257.

Post, D. E. et al. (1978). Computational Studies of Impurity Effects, Impurity Control, and Neutral-Beam Injection in Large Tokamaks. In Plasma Physics and Controlled Nuclear Fusion Research (Proc. 7th Int. Conf. Innsbruck, 1978) 1, IAEA (1979) pp. 471-484.

Rutherford, P. H., S. P. Hirshman, R. Jensen, D. E. Post, F. G. P. Seidl (1976). Impurity

Transport in Tokamaks. In Plasma-Wall Interactions (Proc. Int. Symp. Julich, October, 1976) Pergamon Press, New York (1977) 173.
Schmidt, G. L., N. Bretz, M. Hughes, R. J. Hawryluk, D. W. Johnson and J. A. Schmidt (1977). Density Build-Up in PLT Helium Discharges. Bull. Am. Phys. Soc., paper 8D19, 1180.
Stott, P.E. (1976). Ion Energy Containment in Uncrompressed Discharges in the ATC Tokamak. Plasma Physics 18, 251-263.
Suckewer, S., Hinnov, E., and J. Schivell (1978). Rapid Scanning of Spatial Distribution of Spectral line Intensities in PLT Tokamak. PPPL-1430.
Terry, J. L., E. S. Marmar, K. I. Chen, and H. W. Moos (1977). Observation of Poloidal Asymmetry in Impurity-Ion Emission Due to ∇B Drifts. Phys. Rev. Lett. 39, 1615-1618, 40, 350(e).

DISCUSSION

on paper presented by R. HAWRYLUK

WINSOR

Could I ask for any comments you have on the similarity of Z_{eff} as less than the actual Z of the plasma compared to corresponding deviations of Z_{eff} below the expected value in ALCATOR. In the case of ALCATOR, the toroidal electric field from the ohmic heating becomes a substantial fraction of the runaway field, that is greater than a few per cent. Is there anything corresponding in these cases ?

HAWRYLUK

I have never been able to convince myself of that. The current density in PLT is much smaller. It is hard to see that that would be a problem, though I would be glad to talk to you further about this and see whether we can come to a consensus. I don't see it offhand.

WINSOR

What you have to do really is to correct the runaway field for the number of actual current carriers since we want to trap particles here and it might be comparable.

HAWRYLUK

We should look at that together.

COPPI
A brief comment. As regards some of the questions that you ask, they have, in fact, been resolved by the simulation work done here in Europe over the years. We began, in Bologna, and Garching to simulate the ALCATOR discharges, and when you put together all the various observations there are a rather unique set of diffusion coefficients. For example, let me refer to where you correctly pointed out that if you have an influx of particles, you must have it at the centre. There is a unique expression for the inward flow and now we show that. In particular that flow cannot be related to the temperature gradient, for example, there is a set of experiments in ALCATOR, which shows that, no matter how you vary the temperature gradient, the density gradient does not change. This is similar for the Frascati machine.

HAWRYLUK
A comment about the density gradient. The density gradients in PLT can change quite substantially, especially in going from low to high density discharge.

COPPI
The temperature profile is determined basically by the fusion process as I shall show in my next lecture.

HOGAN
You have stressed the importance of convection to the energy balance. There is a process in which I wonder what your model is which atomic field ..... raised. That is the charge exchange of hydrogen with most of the charged ions. There has been some detailed work by Ralph ISLER of ISX in which he speculated that this process would have to be invoked in a very large ..... to explain the oxygen lines that he was seeing and somebody asked from atomic physics ..... these things are quite large all of them, but he has his measurements ..... any theory. Have you looked at this at all or do you think it might change the convection ..... It really comes in on the neutral - the neutral model that you have used.

HAWRYLUK
A little bit but not enough in detail to say anything quantitative.

GOLDSTON
This is more of an answer to HOGAN's question than anything else. In the beam calculations, we use OLSON and SALOP's calculations of those cross-sections, so that we do have the beam neutral collisions with impurity ions done correctly for the beam penetration. The other question that comes up then is the radiation that the recombined impurity ion makes, and since we do a direct bolometric measurement of the total radiation power that comes in there. Now as far as thermal neutrals charge-exchanging with impurities. I don't think anyone knows the cross-sections in the necessary energy range and we have not made an attempt to include that in the neutral transport code.

PFIRSCH
I have again a question on the Z_{eff} and the bootstrap current. I think that, in principle, the bootstrap current would show up as a reduction in the Z_{eff}.

HAWRYLUK
It's less than a 5% effect for PLT.

PFIRSCH
In principle, there could also be an anomalous bootstrap current related to anomalous transport. You have not analysed what the percentage of this bootstrap current would be ?

HAWRYLUK
You would need something of the order of 20 or 25% if it is true.

(Reviewed by R. HAWRYLUK
and R. GOLDSTON)